Adhesive strength distribution of charged particles on metal substrate in external electric field

AUTHOR(S):

Matsusaka, Shuji; Wei, Dan; Yasuda, Masatoshi; Sasabe, Shuji

Adhesive strength distribution of charged particles on metal substrate in external electric field

Shuji Matsusaka [a,*], Dan Wei [a], Masatoshi Yasuda [a, b], Shuji Sasabe [c]

[a] *Department of Chemical Engineering, Kyoto University, Kyoto 615-8510, Japan*

[b] *IMP, Nara 630-0222, Japan*

[c] *Powder Technology Research Institute, Hosokawa Micron Corporation, Osaka 537-1132, Japan*

Abstract

An improved airflow method to measure the distribution of adhesive strength between charged particles and a metal substrate in an external electric field is presented. In this study, toner particles were negatively charged with a corona charger and deposited on the substrate. The substrate with the particles on the surface was mounted in a rectangular air channel with parallel electrodes. Air velocity was increased at a constant rate, and entrained particles were detected by a laser particle monitor. By studying the relationships between particle entrainment efficiency and air velocity, the particle–substrate adhesion was analyzed in detail. It was found that particle adhesion increased with the increase in the initial charge of particles. It was also found that the particle adhesion increased in a vertically downward electric field but decreased in the upward electric field. These experimental results cannot be explained by the Coulomb force in the electric field. Therefore, a theoretical model based on charge transfer in the external electric field was proposed. This model explains the variation of the particle–substrate adhesion by considering the image force arising due to the transferred charges.

Keywords: Adhesive strength distribution; Charged particle; Metal substrate; External electric field; Airflow method

* Corresponding author. *E-mail address:* matsu@cheme.kyoto-u.ac.jp (S. Matsusaka).

1. Introduction

Powders and particulate solids are widely used in industrial applications. When handled in air, the surfaces of these particles become electrostatically charged by contact or friction with other solid materials. The charged particles cause problems [1, 2] such as adhesion [3-6], segregation [7], as well as fire and explosion hazards [8]. To explain the mechanism of particle charging, several models have been proposed. Some of the proposed models are the condenser model based on contact potential difference [9-11] and the charge relaxation model based on Paschen's law [12-14]. In an electric field, charged particles experience electrostatic forces, making the particles useful in applications such as electrostatic precipitation [15], particle separation [16], powder coating [17], and electrophotography [18]. To achieve an optimum performance in each application, accurate measurement and control of the charge on the particles is crucial [19-23]. In addition, the electrostatic forces acting on the particles need to be measured and analyzed. Several methods, including the centrifuge, electrostatic removal, and micro-cantilever removal have been employed to measure the particle–substrate interaction forces [24-28]; however, simpler and more convenient measurement methods are necessary to enable statistical analysis of the forces.

Theoretical analysis of the charge on particles has been studied for many decades. In a conductive material, the surface charges move until an equilibrium state is attained. In a dielectric material, on the other hand, the charges cannot move freely and remain on the surface; thus, the charges are distributed on the surface according to the charging process. As a typical case, the electrostatic force between a uniformly charged dielectric particle and a conducting plane has been calculated including the effect of higher-order polarizations [29]. The electrostatic force between a partially charged dielectric particle and a conducting particle has

also been calculated, showing that the force strongly depends on the charge distribution [30-32]. When a particle with charge concentrated on its bottom surface is placed on a conducting plane, the electrostatic adhesive force is stronger than that for a uniformly charged particle. The effect of electrostatic behavior of non-uniformly charged particles on a planar dielectric solid has also been investigated [33]. Furthermore, by applying an analytical model for a charged dielectric particle, the attachment and detachment of particles in an applied electric field has been analyzed [34]. In these analyses, the effects of the initial charge of the particle and the applied electric field on the particle–substrate interaction force was studied but the effect of charge transfer by contact between different materials on the interaction force was not studied.

In the present study, we develop an improved experimental method based on particle entrainment to measure the adhesive strength distribution of charged particles in an external electric field, and investigate the effects of the initial charge of particles and the applied electric field on adhesion. The experimental results are discussed taking into account the charge transfer between the surfaces and the image force as well as the Coulomb force.

2. Experiment

2.1 Particle charging and deposition on metal substrate

Fig. 1 shows a schematic diagram of the experimental setup designed for controlling the initial charge of particles and depositing the charged particles on a metal substrate. A small amount of particles were dispersed into airflow through an ejector and negatively charged with a corona charger (Prima Sprint, Wagner-Hosokawa Micron Ltd.). A stainless steel substrate that is 40 mm long, 15 mm wide, and 1 mm high was placed at the distance of 300 mm from the nozzle

of the corona charger. The charged particles were deposited on the substrate in a manner similar to the deposition process used for electrostatic powder coating. The charge on the particles and the amount of particles deposited on the metal substrate were altered by changing the applied voltage and the operation time, respectively. The experimental conditions were as follows: the powder flow rate was 1.0×10^{-5} kg/s and the air flow rate was 1.7×10^{-3} kg/s; thus, the mass flow ratio of the particles to gas was approximately 0.006. The voltage applied to the corona charger was less than 100 kV, and the corona current was less than 120 μA.

2.2. Measurement of adhesive strength distribution of charged particles

Fig. 2 shows a schematic diagram of the experimental setup used for measuring the adhesive strength distribution of charged particles on the metal substrate. The design of this setup is based on the airflow method [35-38]. To analyze the electrostatic forces between particles and the metal substrate in an external electric field, we modified a commercially available airflow system (ASD-01, IMP Co. Ltd.) by adding parallel electrodes. The substrate with the particles prepared in Section 2.1 was manually placed in this system to be mounted flush with the inside surface of a rectangular air channel, which is 1.0 mm high, 8.0 mm wide, and 140 mm long, with an entrance length of 100 mm. A vertical dc electric field was applied in the channel with a high-voltage power supply. The strength and direction of the electric field was controlled in the range of ± 500 kV/m.

Clean compressed dry air was supplied to entrain the particles from the metal substrate. The air velocity in the channel was controlled by a computer and increased at a constant rate. When the separation force caused by aerodynamic drag exceeded the adhesive force, the particles were entrained from the substrate into the airflow. These entrained particles were

detected by a laser particle monitor, in which the airflow rate was kept constant by supplying secondary air. The air flow rate and the output electric signal of the laser particle monitor corresponding to the entrainment flux of particles were automatically recorded into the computer. The measurement time was 10 min, and the data sampling interval was 0.1 s. All the experiments were conducted under room conditions (temperature: 23 ± 5 °C, relative humidity: 28 ± 8%).

2.3 Toner Particles

Toner particles made of polyester were used in this experiment. Toner A was free of external additives, whereas toner B was modified with external additives; i.e. polyester particles were coated with silica nanoparticles to decrease the adhesive forces. This is because the nanoroughness created by the silica nanoparticles on the surface of the polyester particles decrease the adhesive forces.

Fig. 3 shows the SEM images of these toner particles. It is found that the shape of the particles is irregular, and the two types of toner particles are similar to each other in shape and size. Fig. 4 shows count-based particle size distributions. There was no notable difference between the two types of particles. The values of the count median diameter, D_{p50}, and the geometric standard deviation, σ_g, were 5.6 μm and 1.3, respectively. Table 1 summarizes the properties of these toner particles.

2.4 Analysis method of particle–substrate adhesion

As the particle–substrate adhesion depends on each contact state, the adhesive force is not constant; thus, the air velocity for particle entrainment is distributed. The distribution function can be analyzed by the particle entrainment efficiency, η, which is defined as the number ratio of entrained particles to total particles [36, 37], i.e.:

$$\eta = \frac{\int_0^u n' du}{\int_0^\infty n' du}, \tag{1}$$

where n' is the differential coefficient of the number of entrained particles with respect to the cross-sectional average air velocity, u.

3. Results and discussion

3.1. Electrostatic charging and particle deposition on metal substrate

The toner particles, which tend to be charged negatively by contact with a wall, were more negatively charged by the corona charger and the charge-to-mass ratio, namely specific charge, was measured using a Faraday cup. Fig. 5 shows the relationship between specific charge, q_{m0}, and corona voltage, V. As the corona voltage increases, the specific charge increases. This experimental result indicates that the particle charge can be controlled by the corona voltage.

The amount of the charged particles deposited on the substrate was controlled by changing the amount of supplied particles, and the particle deposition density on the substrate was in the range of 2.1 ± 0.4 g/m^2. Fig. 6 shows the image of toner A deposited on the substrate that was obtained through an optical microscope. It is found that the particles were well distributed on the substrate. Since the particles have different shapes and sizes, the values of particle–substrate

adhesion will be distributed. Therefore, the measurement of the distribution is important.

3.2. Particle entrainment

Fig. 7 shows a typical experimental result for particle entrainment. The upper graph shows the variation of the air velocity in the channel where the air velocity increases up to 300 m/s in 600 s at a constant rate of 0.5 m/s^2. The lower graph shows a particle entrainment profile as a function of time elapsed, where V_s is the output electric signal of the laser particle monitor that corresponds to the particle entrainment flux. Although there are fluctuations in the data, the particles begin to entrain at a certain air velocity, and the quantity of the particles entrained from the substrate into the airflow increases with time but finally decreases with decreasing amount of particles on the substrate. When the time is 50 s, air velocity is 25 m/s and the Reynolds number is 3000. Therefore, almost all the particles entrain in turbulent flow. In the measurement, the particle entrainment caused by the collision of entrained particles seldom occurs. This is because the particles are carried toward the main flow immediately after the detachment from the substrate [37].

The particle entrainment profile depends on the experimental conditions such as the initial charge of particles and the external electric field. To analyze the particle entrainment profile, we used the cumulative distribution function, which was obtained by summing the digital data and dividing by the sum of the total digital data. As a result, the fluctuations in the data were removed and the feature of the particle entrainment efficiency was clearly visible.

3.3. Effect of initial charge on particle entrainment efficiency

Fig. 8 shows the relationships between particle entrainment efficiency, η, and air velocity, u, as a function of the initial charge of particles, q_{m0}. These results were obtained under the condition of no external electric field. Particle entrainment efficiency increases with air velocity. The entrainment efficiency curves shift toward higher air velocities with the increase in the amount of initial charge. In order to evaluate the effect of initial charge on particle entrainment, we focus on the median value of air velocity, u_{50}, at which 50% of the particles are entrained, hereafter called as entrainment velocity.

Fig. 9 shows the effect of the initial charge of particles, q_{m0}, on entrainment velocity, u_{50}. The entrainment velocity of particles increases with the increase in the amount of the initial charge; i.e. the particle–substrate adhesion increases with increasing initial charge. When the applied voltage is zero, there is no Coulomb force caused by the external electric field. However, when the particles have initial charges, image charges are induced in the substrate; subsequently, the image force enhances the adhesive force.

3.4. Effect of external electric field on particle entrainment efficiency

Fig. 10(a) shows the relationships between particle entrainment efficiency and air velocity as a function of the external electric field. The experimental results were obtained using toner A with an initial charge of –28 mC/kg. When the substrate acts as the negative electrode, the direction of the external electric field is downward. In this case, we assume that the electric field is negative. The entrainment efficiency curves tend to shift toward higher air velocities with the increase in the strength of this negative electric field. On the other hand, for a positive electric field, the entrainment efficiency curves tend to shift toward the opposite direction with the strength of the electric field. These experimental results indicate that the particle–substrate

adhesion increases in the negative electric field but decreases in the positive electric field. Fig. 10(b) shows the results for highly negatively charged particles (q_{m0} = –38 mC/kg). The effect of the external electric field on entrainment efficiency is qualitatively similar to that in Fig. 10(a), but the entrainment efficiency curves tend to shift toward much higher air velocities.

Fig. 11 shows the effect of the external electric field, E, on entrainment velocity, u_{50}, which was obtained from the experimental data shown in Fig. 10. The entrainment velocity linearly decreases with the increase in the external electric field. In addition, the value of the entrainment velocity increases with the initial charge.

Fig. 12 shows the entrainment efficiency curves for toner B, whose surface was modified with silica nanoparticles to reduce particle–substrate adhesion. The effect of the external electric field on entrainment velocity is similar to that for toner A although the values of the entrainment velocity are rather small compared to that of toner A.

Fig. 13 shows the effect of the external electric field on entrainment velocity that was obtained from the experimental data shown in Fig. 12. The entrainment velocity decreases with the increase in the external electric field and increases with the increase in the initial charge. The tendency of the electrostatic force is similar to that shown in Fig. 11. From the above experimental results, it was found that the external electric field and initial charge are the main factors that affect particle–substrate adhesion.

3.5. Discussion of electrostatic forces acting on particles

A charged particle on the metal surface experiences various particle–substrate interaction forces, including the van der Waals force, electrostatic force, and gravity. However, the experimental results showed that the electrostatic force was significant, i.e. particle charge and

external electric field greatly affected particle–substrate adhesion. The charged particles on the substrate experience image and Coulomb forces in the external electric field. The Coulomb force, $F_{E,}$ is represented by the following equation:

$$F_E = E\ q\ , \tag{2}$$

where E is the electric field strength and q is the particle charge. The direction of the Coulomb force depends on the polarity of the particle charge and the direction of the electric field; i.e. the Coulomb force can be attractive or repulsive for the particle–substrate interaction.

The image force, F_I, is represented by the following equation:

$$F_I = -k\,q^2 \tag{3}$$

and

$$k = \frac{1}{4\pi\,\varepsilon_0\,d^2}, \tag{4}$$

where q is a virtual point charge, ε_0 is the permittivity of air, and d is the distance. The image force is always attractive for the particle–substrate interaction irrespective of the polarity of the particle charge.

When the direction of the external electric field is downward, in which case the electric field is assumed to be negative, the Coulomb force acting on the negatively charged particle must be repulsive for the particle–substrate interaction. On the other hand, when the external electric field is positive, the Coulomb force must be attractive. Therefore, the Coulomb force weakens the particle–substrate adhesion in the negative electric field but strengthens the particle–substrate adhesion in the positive electric field. The experimental results in Section 3.4,

however, showed the opposite. To explain the experimental results, we need to consider other factors.

3.6. A model including the effect of charge transfer in external electric field

When two different materials are brought into contact and separated, an electric charge is transferred from one to the other owing to the potential difference. This phenomenon is called contact charging [1, 2]. A typical charge-transfer model is known as the condenser model, and the total potential difference, V, at the contact gap is expressed as:

$$V = V_{\mathrm{c}} - V_{\mathrm{e}} + V_{\mathrm{ex}}, \tag{5}$$

where V_{c} is the contact potential difference that depends on surface work functions, V_{e} is the potential difference owing to the image charge, and V_{ex} is the potential difference caused by the external electric field. The contact potential difference V_{c} is expressed as

$$V_c = -\frac{\varphi_{\mathrm{p}} - \varphi_{\mathrm{s}}}{e}, \tag{6}$$

where φ_{p} and φ_{s} are the work functions of the particle and the substrate, respectively, and e is the elementary charge.

Fig. 14 shows a charge-transfer model based on the total potential difference in which the contact potential difference, V_{c}, was assumed to be negative. The charge transfer depends on the particle charge and the external electric field [22, 23]. For example, when the external electric field, E_{ex}, is applied negatively in this system, the total potential difference, V, becomes largely negative and the transferred charge, Δq, from the substrate to the particle is also negative. On the other hand, a positive electric field causes a positive potential difference and a positive

charge is transferred from the substrate to the particle. The transferred charge will affect the particle–substrate interaction.

Fig. 15 illustrates the variations of the electrostatic forces acting on the negatively charged particle placed on the metal substrate. When the external electric field, E_{ex}, is applied negatively, negative charge is transferred from the substrate to the particle and the amount of the total charge on the particle increases. Although the Coulomb force caused by the external electric field reduce the particle–substrate adhesion, the image force greatly increases the adhesion because the transferred charge is accumulated around the contact area. On the other hand, the positive external electric field reduces the negative charge on the particle, particularly the surface around the contact area. Although the Coulomb force can act as the attractive force for the particle–substrate interaction, the image force is greatly reduced; thus, the adhesive force decreases. As mentioned above, the variation of the particle–substrate adhesion can be well explained by the model taking into account the charge transfer caused by the external electric field and the image force.

4. Conclusions

Adhesive strength distribution of charged particles in an external electric field was measured by an improved airflow method, and the effects of the initial charge of particles and external electric field on the particle–substrate adhesion was investigated in detail. The results obtained experimentally and theoretically are summarized as follows:

1) The particle–substrate adhesion increases with the increase in the amount of initial charge with no external electric field. This is because an image charge is induced in the substrate and the image force enhances the particle–substrate adhesion.

2) A charged particle in an external electric field has a Coulomb force, which varies depending on the polarity and the amount of particle charge as well as the direction and strength of the external electric field; thus, the Coulomb force can be attractive or repulsive for the particle–substrate interaction. This is theoretically true. However, experimental results showed that the adhesive force acting on negatively charged particles increased in a vertically downward electric field and decreased in an upward electric field. These results cannot be explained by the Coulomb force in the external electric field.

3) When applying an external electric field, charge is transferred between the particle and substrate according to the total potential difference at the contact gap. The transferred charge around the contact area greatly changes the image force, which affects the particle–substrate adhesion. The proposed theoretical model can thus explain the variation of the particle–substrate adhesion.

Acknowledgement

This research was supported in part by Grant-in-Aid for Scientific Research (B) (No. 26289288) from the Japan Society for the Promotion of Science.

References

[1] S. Matsusaka, H. Masuda, Electrostatics of particles. Adv. Powder Technol. 14 (2003) 143–166.

[2] S. Matsusaka, H. Maruyama, T. Matsuyama, M. Ghadiri, Triboelectric charging of powders:

a review, Chem. Eng. Sci. 65 (2010) 5781–5807.

[3] I. Adhiwidjaja, S. Matsusaka, S. Yabe and H. Masuda, Simultaneous phenomenon of particle deposition and reentrainment in charged aerosol flow —effects of particle charge and external electric field on the deposition layer, Adv. Powder Technol. 11 (1999) 221–233.

[4] J. Yao, Y. Zhang, C.-H. Wang, S. Matsusaka, H. Masuda, Electrostatics of the granular flow in a pneumatic conveying system. Ind. Eng Chem. Res. 43 (2004) 7181–7199.

[5] F.Y. Leong, K. A. Smith, C.-H. Wang, S. Matsusaka, J. Hua, Electrostatic effects on inertial particle transport in bifurcated tubes. AIChE J. 55 (2009) 1390-1401.

[6] E.W.C. Lim, Mixing behaviors of granular materials in gas fluidized beds with electrostatic effects, Ind. Eng. Chem. Res. 52 (2013) 15863–15873

[7] E. Šupuk, A. Hassanpour, H. Ahmadian, M. Ghadiri1, T. Matsuyama, Tribo-electrification and associated segregation of pharmaceutical bulk powders, KONA Powder and Particle J. 29 (2011) 208–223

[8] T.B. Jones, J.L. King, Powder Handling and Electrostatics: Understanding and Preventing Hazards, Lewis, Chelsea. (1991)

[9] B.N. Cole, M.R. Baum, F.R. Mobbs, An investigation of electrostatic charging effects in high-speed gas–solids pipe flows. P. I. Mech. Eng. 184 (1969–1970) 77–83.

[10] H. Masuda, T. Komatsu, K. Iinoya, The static electrification of particles in gas–solids pipe flow. AIChE J. 22 (1976) 558–564.

[11] S. Matsusaka, M. Ghadiri, H. Masuda, Electrification of an elastic sphere by repeated impacts on a metal plate. J. Phys. D: Appl. Phys. 33 (2000) 2311–2319.

[12] T. Matsuyama, H. Yamamoto, Charge relaxation process dominates contact charging of a particle in atmospheric conditions. J. Phys. D: Appl. Phys. 28 (1995a) 2418–2423.

[13] T. Matsuyama, H. Yamamoto, Characterizing the electrostatic charging of polymer particles by impact charging experiments. Adv. Powder Technol. 6 (1995b) 211–220.

[14] T. Matsusyama, H. Yamamoto, Impact charging of particulate materials. Chem. Eng. Sci. 61 (2006) 2230–2238.

[15] A. Mizuno, Electrostatic Precipitation, IEEE T. Dielect. El. In. 7 (2000) 615–624

[16] G.Q. Wu, J. Li, Z.M. Xu, Triboelectrostatic separation for granular plastic waste recycling: a review, Waste Manage., 33 (2013) 585–597.

[17] W. Kleber, B. Makin, Triboelectric powder coating: a practical approach for industrial use, Particul. Sci. Technol. 16 (1998) 43–53.

[18] L.B. Schein, Electrophotography and Development Physics, 2nd ed. Springer-Verlag, Berlin/ Laplacian Press, 1992/1996.

[19] S. Matsusaka, T. Nishida, Y. Gotoh, H. Masuda, Electrification of fine particles by impact on a polymer film target, Adv. Powder Technol. 14 (2003) 127–138.

[20] S. Matsusaka, M. Oki, H. Masuda, Control of electrostatic charge on particles by impact charging, Adv. Powder Technol. 18 (2007) 229–244.

[21] S. Matsusaka, H. Fukuda, Y. Sakura, H. Masuda, M. Ghadiri, Analysis of pulsating electric signals generated in gas-solids pipe flow, Chem. Eng. Sci. 63 (2008) 1353–1360.

[22] S. Matsusaka, Control of particle tribocharging, KONA Powder Part. J. 29 (2011) 27–38.

[23] P. Bunchatheeravate, J. Curtis, Y. Fujii, S. Matsusaka, Prediction of particle charging in a dilute pneumatic conveying system, AIChE J. 59 (2013) 2308–2316.

[24] B. Gady, D. Schleef, R. Reifenberger, Identification of electrostatic and van der Waals interaction forces between a micrometer-size sphere and a flat substrate, Phys. Rev. B 53 (1996) 8065–8070

[25] H. Mizes, M. Ott, E. Eklund, D. Hays, Small particle adhesion: measurement and control, Colloid Surface A 165 (2000) 11–23.

[26] M. Takeuchi, Adhesive forces of charged particles, Chem. Eng. Sci. 61 (2006) 2279–2289.

[27] T. Matsuyama, M. Ohtsuka, H. Yamamoto, Measurement of force curve due to electrostatic charge on a single particle using atomic force microscope, KONA Powder Part. J. 26 (2008) 238–245.

[28] J.W. Kwek, I.U. Vakarelski, W.K. Ng, J.Y.Y. Heng, R.B.H. Tan, Novel parallel plate condenser for single particle electrostatic force measurements in atomic force microscope, Colloids Surf., A 385 (2011) 206–212.

[29] T. Matsuyama, H. Yamamoto, The electrostatic force between a charged dielectric particle and a conducting plane, KONA Powder Part. J. 16 (1998) 223–227.

[30] T. Matsuyama, H. Yamamoto, The electrostatic force between a partially charged dielectric particle and a conducting plane, Part. Part. Syst. Charact. 24 (2007) 1–6.

[31] B. Techaumnat and T. Takuma, Analysis of the electrostatic force on a dielectric particle with partial charge distribution, J. Electrost. 67 (2009) 686–690.

[32] B. Techaumnat, M. Kadonaga, and T. Takuma, Analysis of electrostatic adhesion and detachment of a nonuniformly charged particle on a conducting plane, IEEE T. Dielect. El. In. 16 (2009) 704–709.

[33] B. Techaumnat, M. Kadonaga, Electrostatic force behavior of a nonuniformly charged particle on a planar dielectric solid, IEEE T. Dielect. El. In. 18 (2011) 1366–1373

[34] B. A. Kemp, J. G. Whitney, Nonlinear nature of micro-particle detachment by an applied static field, Appl. Phys. Lett. 102 (2013) 141605

[35] H. Masuda, S. Matsusaka, K. Imamura, A new method for measurement of powder characteristics based on reentrainment phenomena, KONA Powder Part. J. 12 (1994) 133–143.

[36] Y. Jiang, S. Matsusaka, H. Masuda, T. Yokoyama, Characterizing the effect of surface morphology on particle–wall interaction by the airflow method, Adv. Powder Technol. 17, (2006) 413–424.

[37] Y. Jiang, S. Matsusaka, H. Masuda, Y. Qian, Characterizing the effect of substrate surface roughness on particle–wall interaction with the airflow method, Powder Technol. 186 (2008), 199–205.

[38] K. Toizumi, Y. Shibai, T. Nakamura, S. Matsusaka, Measurement of adhesive strength distribution between toner and carrier particles by airflow method, J. Imaging Soc. Jpn. 49 (2010) 154–158.

Table 1. Properties of the two types of toner particles.

Sample	Resin	D_{p50} (μm)[a]	σ_g (–)[b]	Shape	External additive
Toner A	Polyester	5.6	1.3	Irregular	Free
Toner B	Polyester	5.6	1.3	Irregular	Silica nanoparticles

[a] D_{p50}: count median diameter.

[b] σ_g: geometric standard deviation of particle diameter.

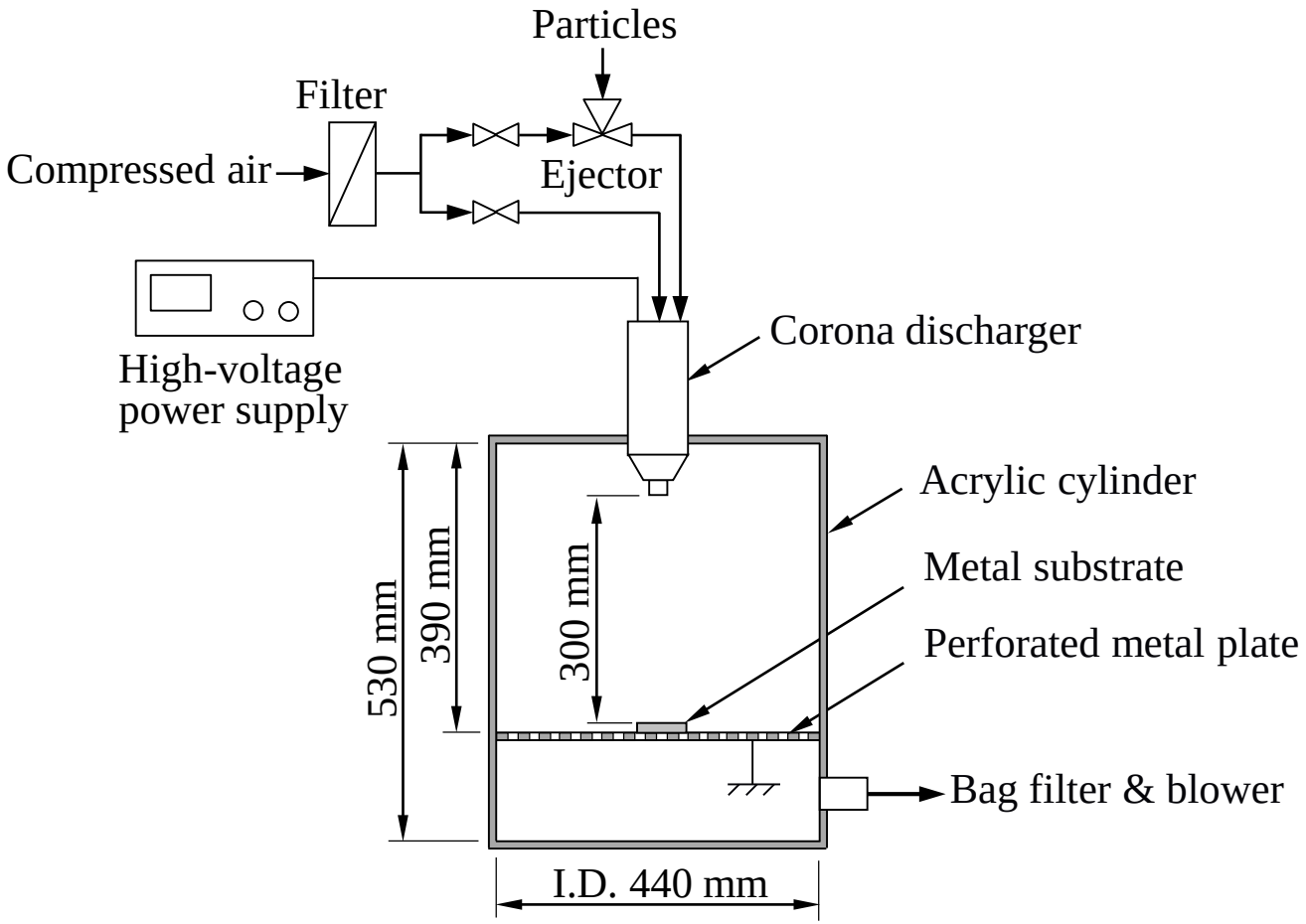

Fig. 1. Experimental setup for controlling the initial charge of particles and depositing the charged particles on a metal substrate.

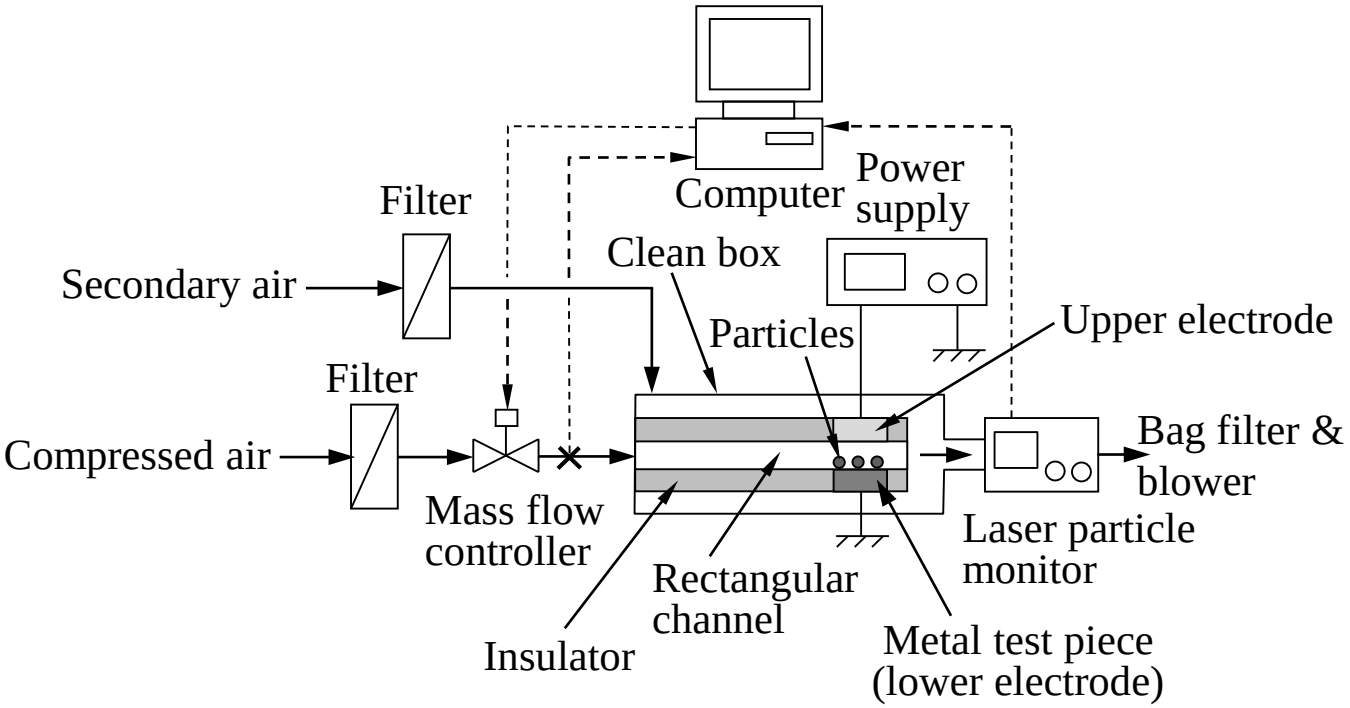

Fig. 2. Experimental setup for measuring particle–substrate adhesion.

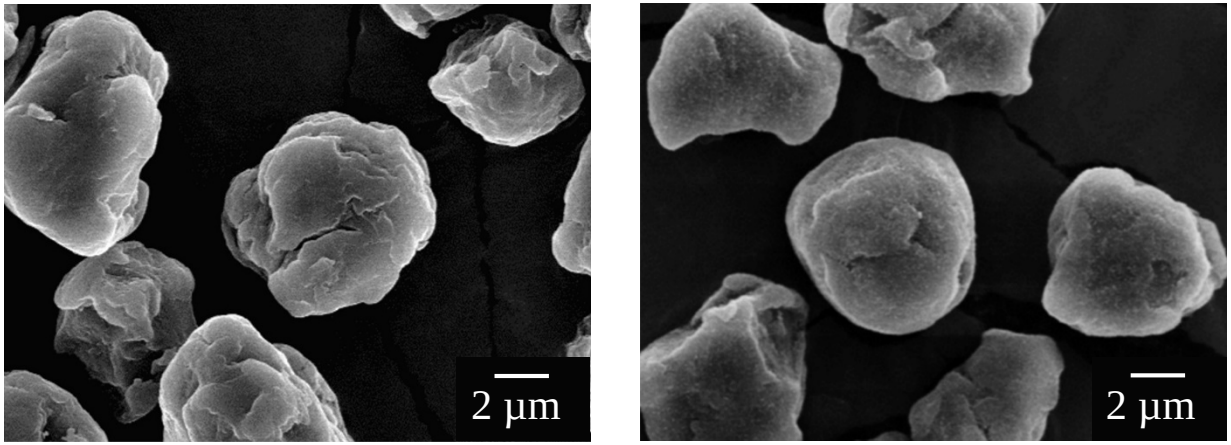

(a) Toner A (b) Toner B

Fig. 3. SEM images of toner particles.

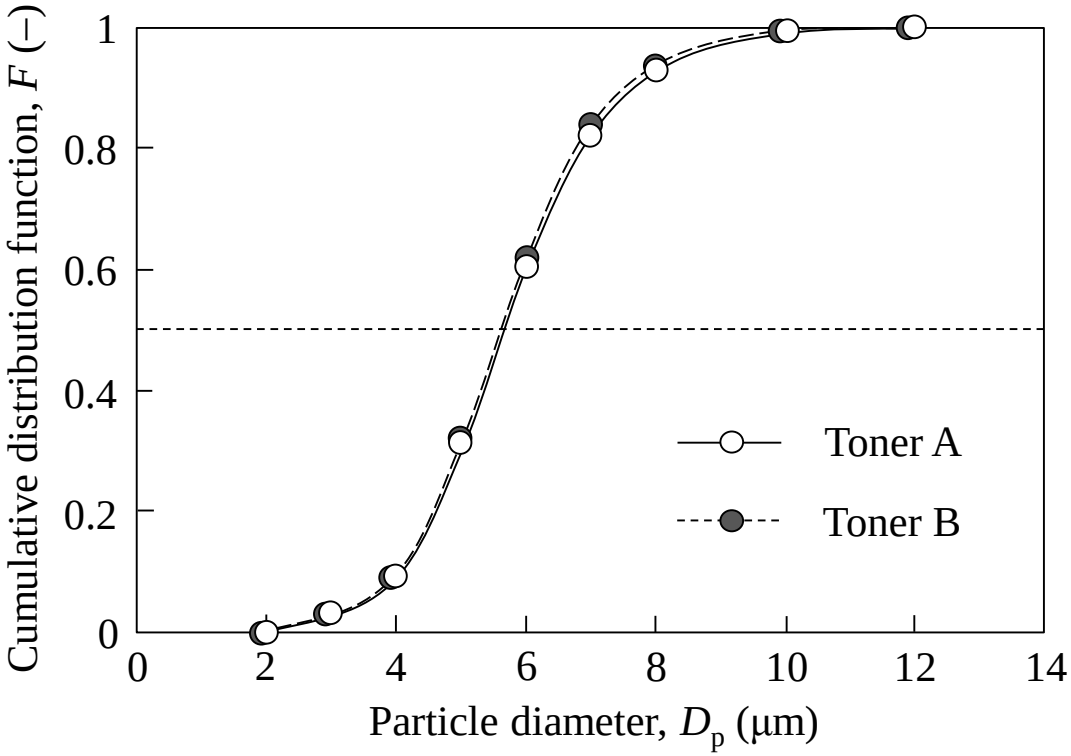

Fig. 4. Count-based particle size distributions.

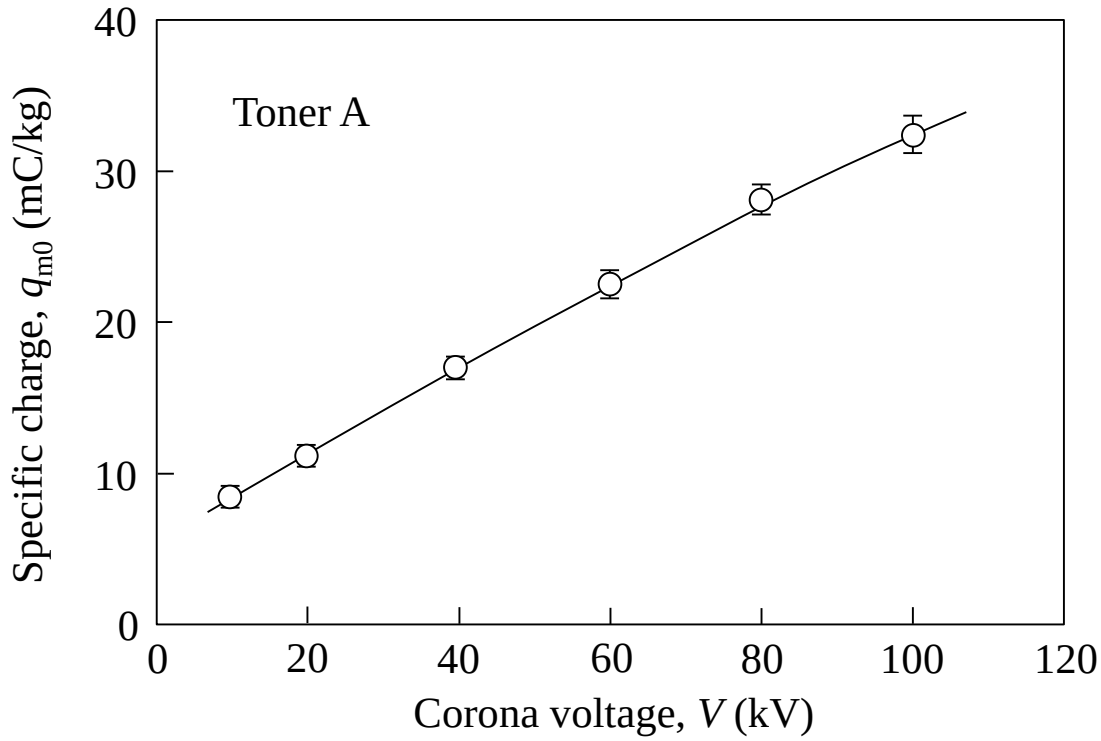

Fig. 5. Relationship between specific charge and corona voltage (q_{m0} is negative).

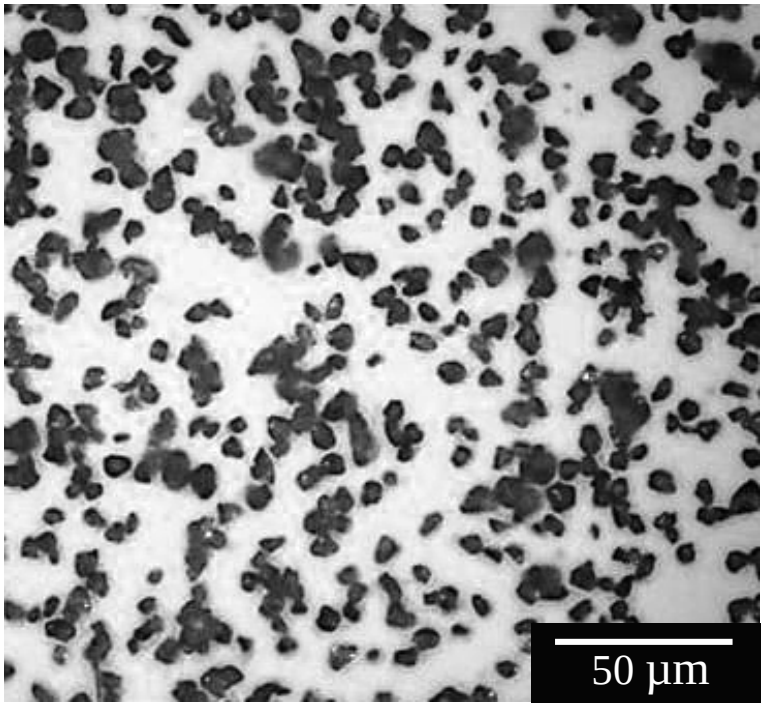

Fig. 6. Images of particles deposited on the substrate (toner A, particle deposition density on the substrate: 1.7 g/m^2).

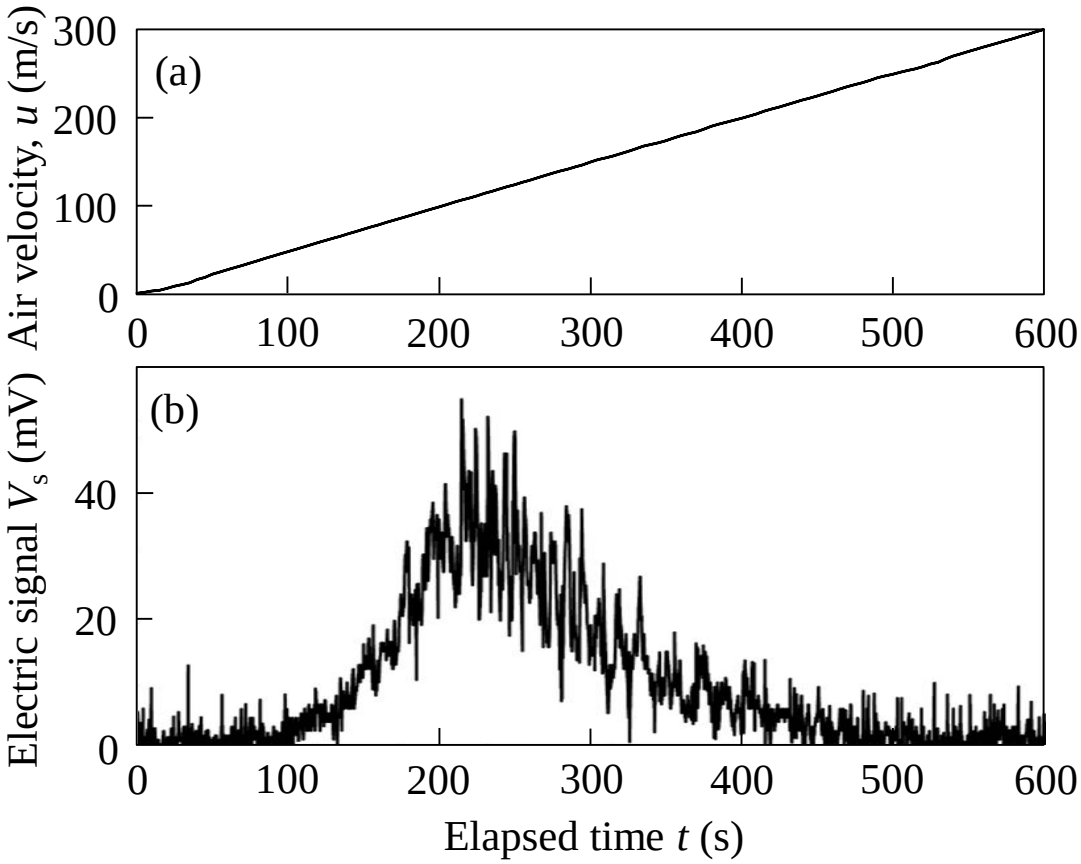

Fig. 7. Experimental result for toner A: (a) variation of air velocity in the channel; (b) particle entrainment profile (deposition density on the substrate: 1.8 g/m^2, initial charge: –37 mC/kg, external electric field: +300 kV/m).

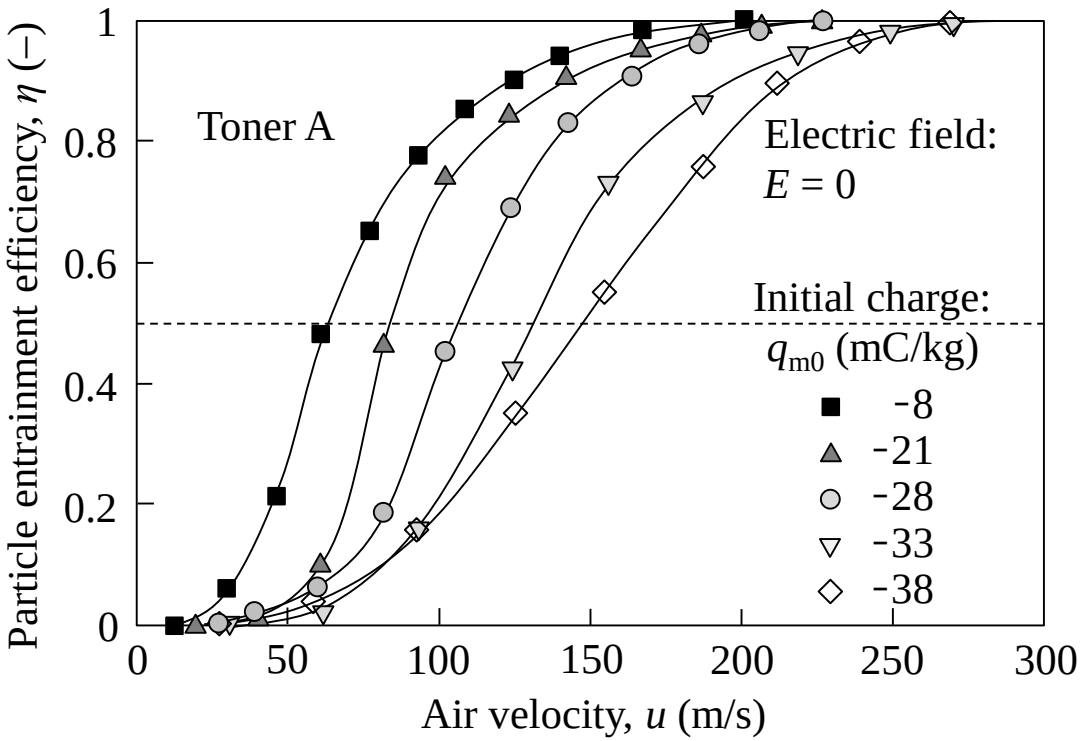

Fig. 8. Relationships between particle entrainment efficiency and air velocity as a function of the initial charge of particles.

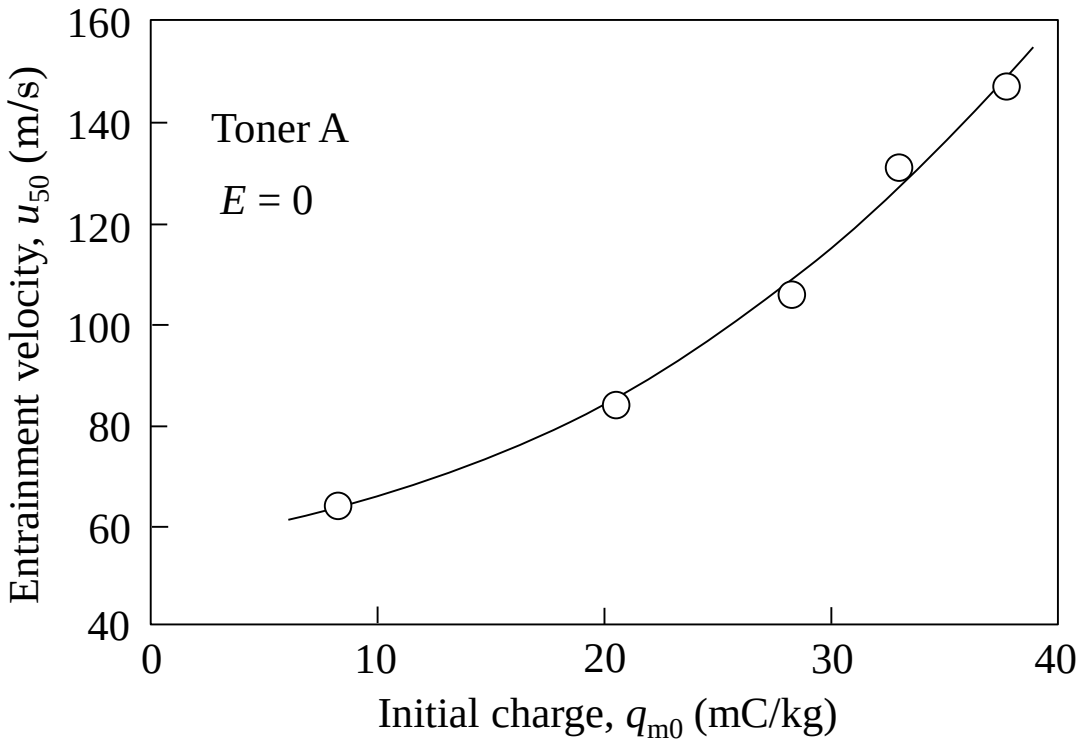

Fig. 9. Effect of the initial charge of particles on entrainment velocity (q_{m0} is negative).

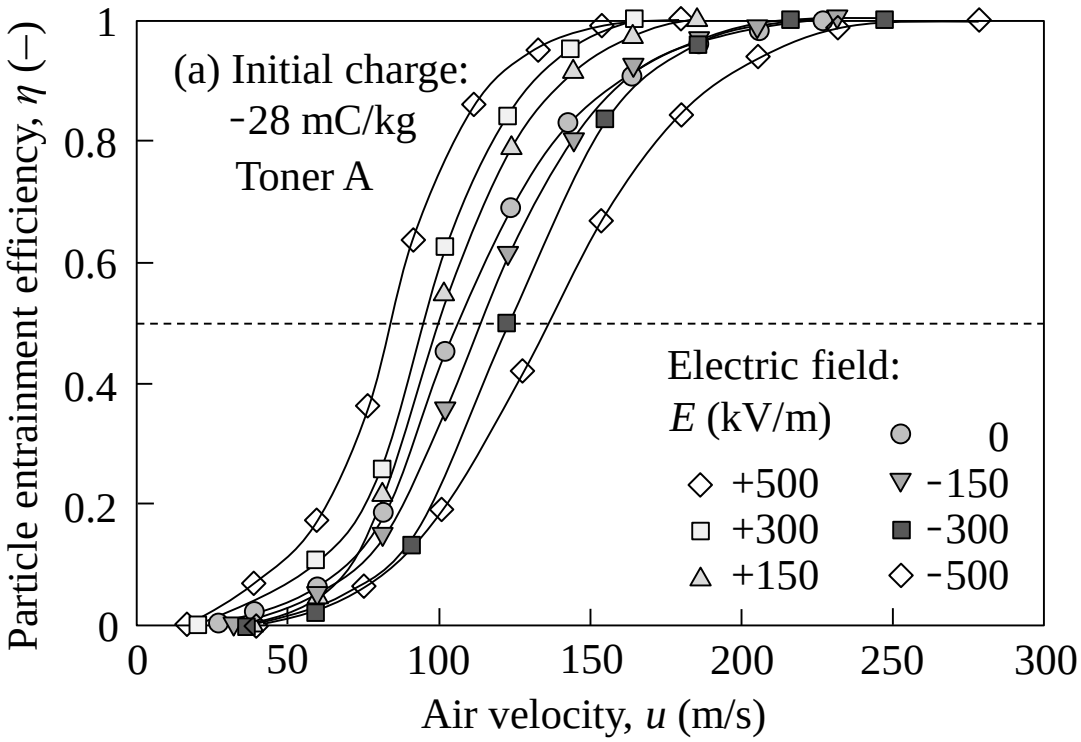

Fig. 10. Relationships between particle entrainment efficiency and air velocity as a function of the external electric field (Toner A).

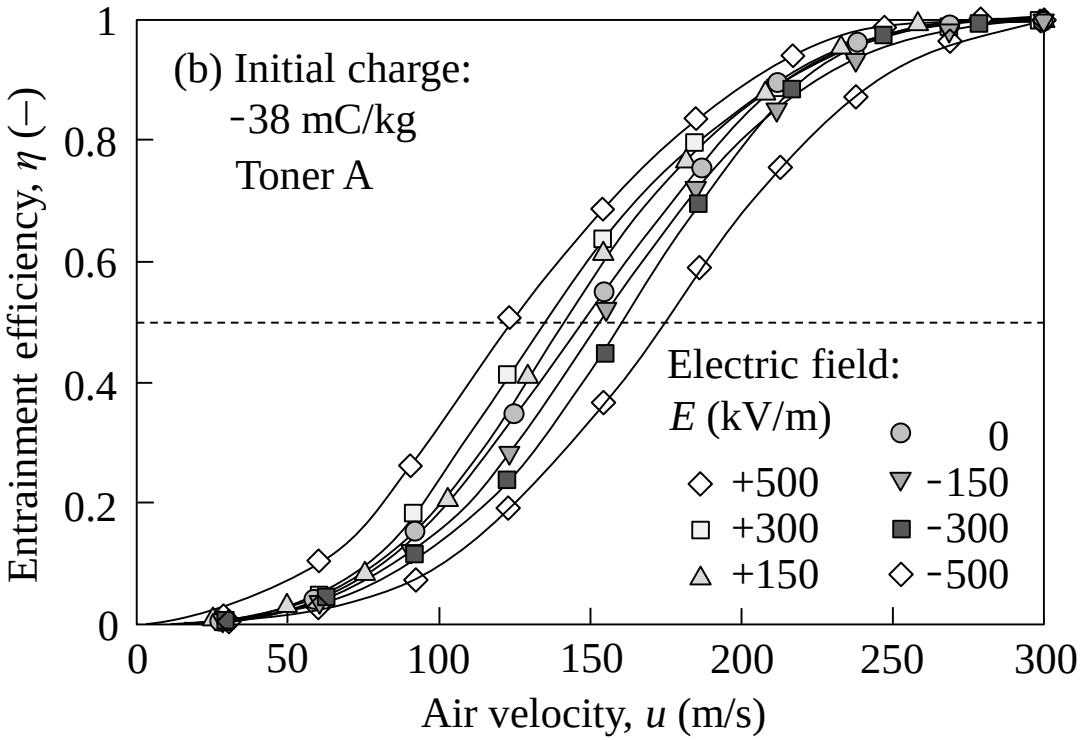

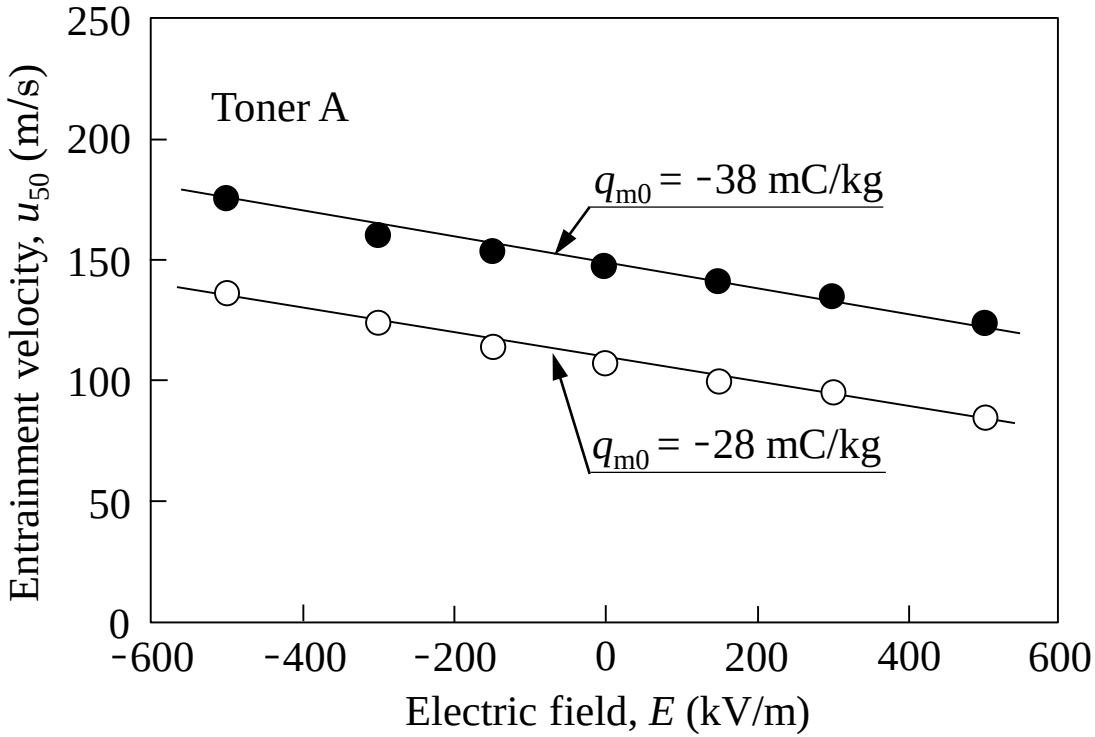

Fig. 11. Effect of external electric field on entrainment velocity (Toner A).

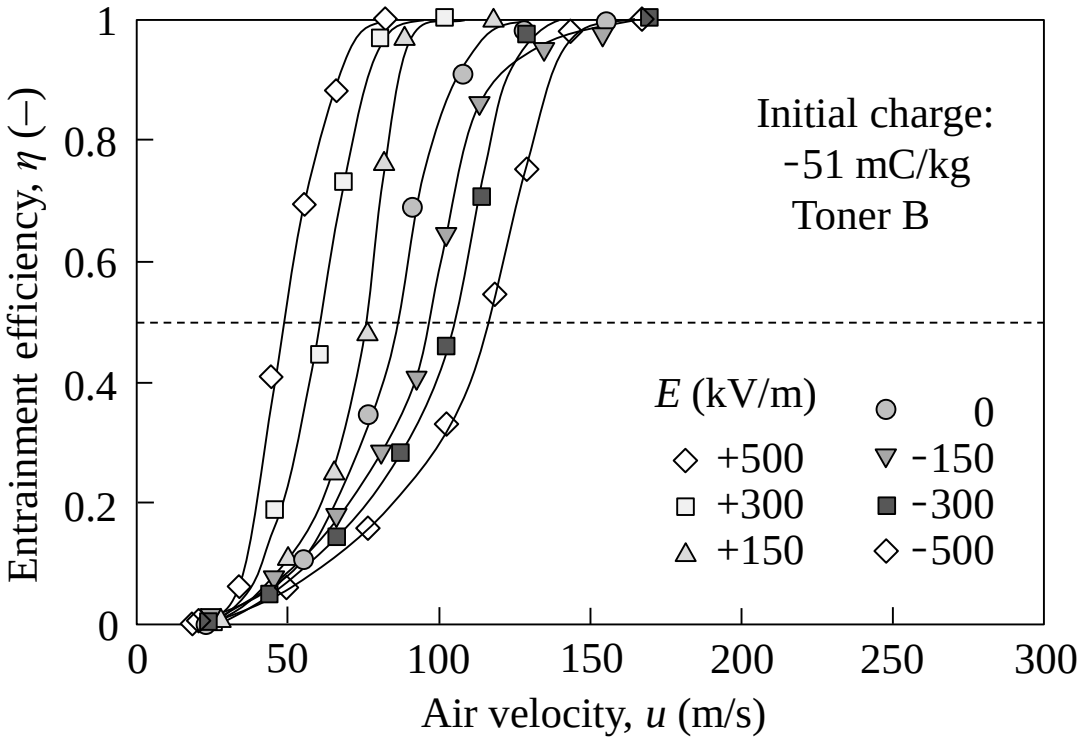

Fig. 12. Entrainment efficiency curves for Toner B.

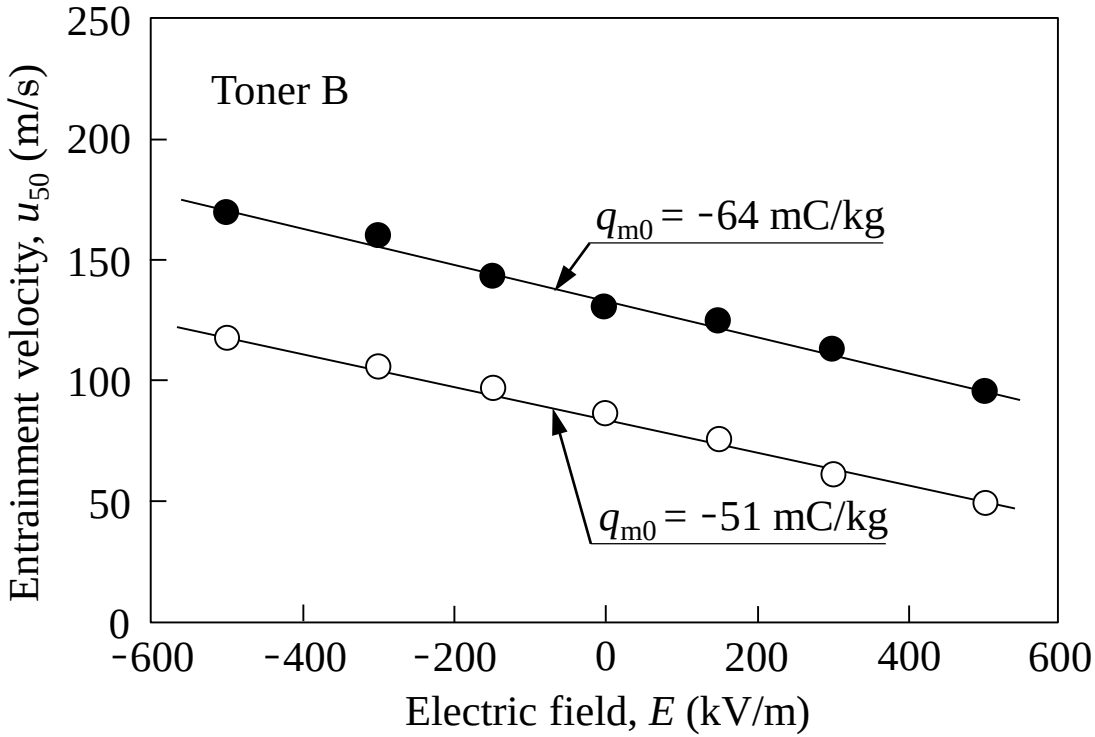

Fig. 13. Effect of external electric field on entrainment velocity (Toner B).

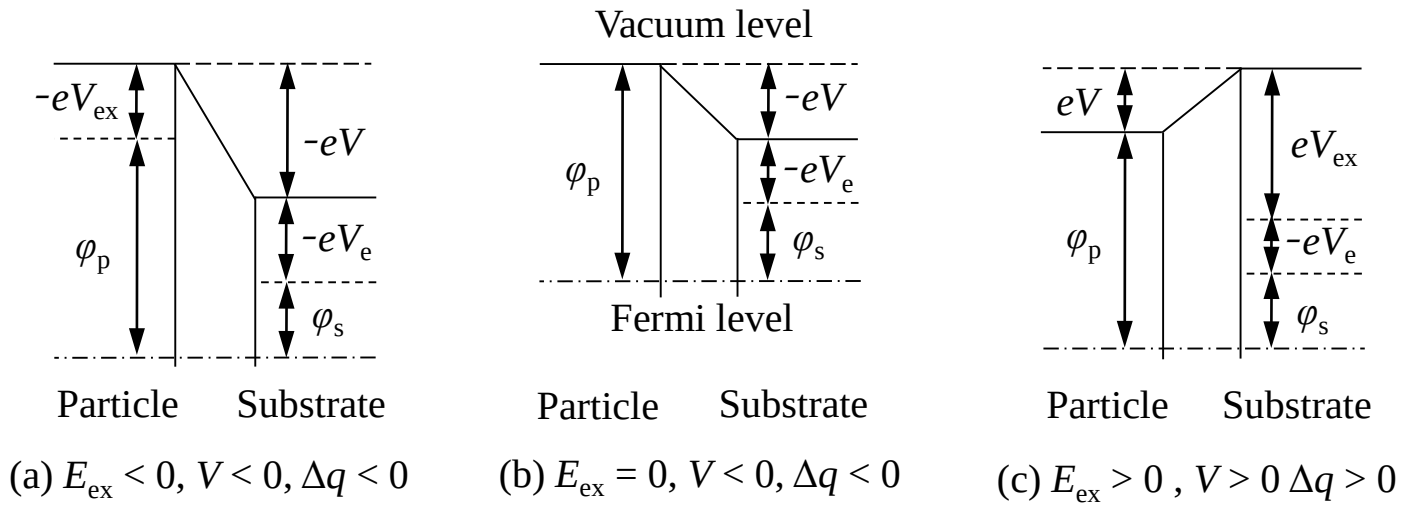

Fig. 14. A charge-transfer model based on the total potential difference (V: total potential difference, V_{ex}: potential differences caused by external electric field, V_e: potential differences caused by image charge, e: elementary charge, φ: work function, E_{ex}: external electric field, Δq: charge transferred from the substrate to the particle based on the total potential difference).

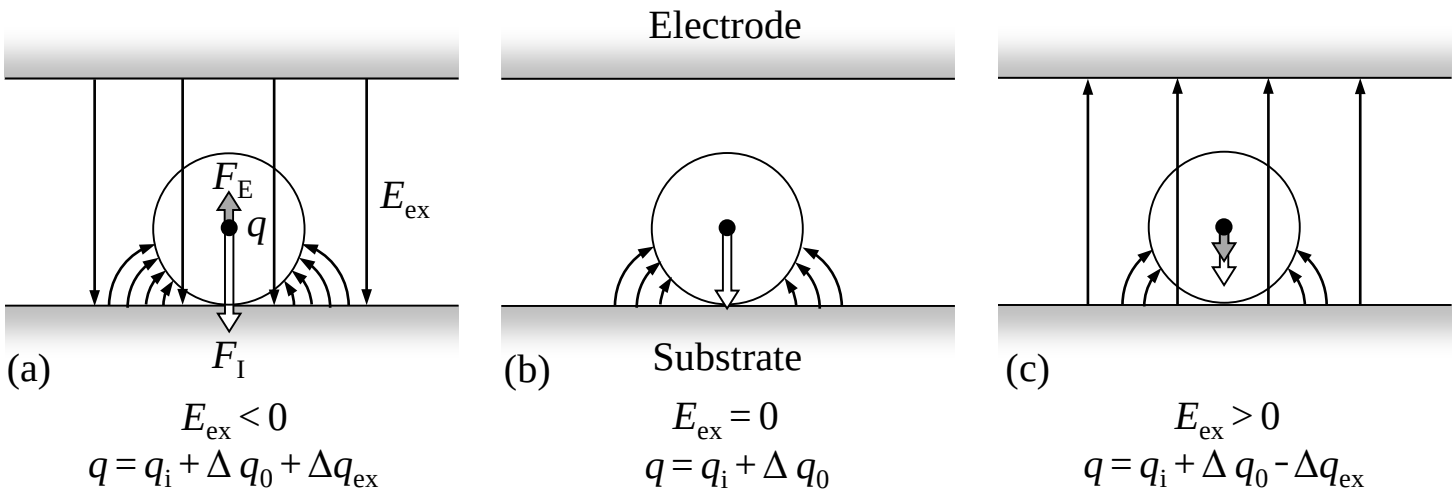

Fig. 15. Image force F_I and Coulomb force F_E in an external electric field E_{ex} (q: particle charge, q_i: initial charge, Δq_0: charge transferred without external electric field, Δq_{ex}: charge transferred caused by external electric field, $q_i < 0$, $\Delta q_0 < 0$, $\Delta q_{ex} < 0$).